

Stability Analysis using Quadratic Constraints for Systems with Neural Network Controllers

He Yin, Peter Seiler and Murat Arcak

Abstract—A method is presented to analyze the stability of feedback systems with neural network controllers. Two stability theorems are given to prove asymptotic stability and to compute an ellipsoidal inner-approximation to the region of attraction. The first theorem addresses linear time-invariant plant dynamics, and merges Lyapunov theory with local (sector) quadratic constraints to bound the nonlinear activation functions in the neural network. The second theorem allows the plant dynamics to include perturbations such as unmodeled dynamics, slope-restricted nonlinearities, and time delay, using integral quadratic constraint (IQCs) to capture their input/output behavior. Both results rely on semidefinite programming to compute Lyapunov functions and inner-estimates of the region of attraction. The method is illustrated on systems with neural networks trained to stabilize a nonlinear inverted pendulum as well as vehicle lateral dynamics with actuator uncertainty.

I. INTRODUCTION

The paradigm of stabilizing dynamical systems with Neural Network (NN) controllers [1] has been revived following recent development in deep NNs, e.g. policy gradient [2]–[5] and behavioral cloning [6]. However, feedback systems with NN controllers suffer from lack of stability and safety certificates due to the complexity of the NN structure. Specifically, NNs have various types of nonlinear activation functions, potentially numerous layers, and a large number hidden neurons, making it difficult to apply classical analysis methods, e.g. Lyapunov theory [7], [8]. Monte-Carlo simulations can be used to investigate stability but lack formal guarantees, which are important in safety-critical applications such as aircraft and space launch vehicles.

Several works propose using quadratic constraints (QCs) to bound the nonlinear activation functions. This approach is used to outer-bound the outputs of a (static) NN given a set of inputs in [9] and upper-bound the Lipschitz constant of NNs in [10], [11]. The work [12] uses this idea for finite-time reachability analysis of a system with a NN controller. References [13], [14] approximate NN functions with polynomials, while [15] proposes a verification method that transforms sigmoid-based NNs into equivalent hybrid systems. The work [16] performs stability analysis by constructing QCs from the bounds of partial gradients of NN controllers. Reference [17] assesses global asymptotic stability of dynamic neural network models using QCs and Lyapunov theory.

This paper presents two main stability results for a feedback system with a NN controller. Theorem 1 provides a condition

to prove stability and to inner-estimate the region of attraction for a linear time-invariant (LTI) plant. It uses Lyapunov theory, and local (sector) QCs to bound the nonlinear activation functions in the NN. Theorem 2 allows the plant to include perturbations such as unmodeled dynamics, slope-restricted nonlinearities, and time delay, characterizing them with integral quadratic constraints (IQCs) [18], [19]. Both results rely on semidefinite programming to compute Lyapunov functions and inner-estimates of the region of attraction.

The specific contributions of this paper are two-fold. First, our nominal analysis with LTI plants and NN controllers uses local sector QCs that provide tight regional bounds and avoid the conservatism of the global constraints used in [9]–[12], [17]. This allows us to provide stability certificates and region of attraction estimates when global stability tests are infeasible. Moreover, our approach derives local QCs for activation functions using bounds only on the input to the first layer. This differs from [16] which derives bounds using partial gradients of the activation functions. Second, our analysis of uncertain plants and NN controllers provides robustness guarantees for the feedback system. The uncertain plant is modeled as an interconnection of the nominal plant and perturbations that are described by IQCs. The use of IQCs also allows for plants that are not necessarily LTI.

The paper is organized as follows. Section II presents the problem formulation and the nominal stability analysis when the plant is LTI. Section III addresses uncertain systems using IQCs. Section IV provides numerical examples, including a nonlinear inverted pendulum example and an uncertain vehicle lateral control example. Section V summarizes the results.

Notation: \mathbb{S}^n denotes the set of n -by- n symmetric matrices. \mathbb{S}_+^n and \mathbb{S}_{++}^n denote the sets of n -by- n symmetric, positive semidefinite and positive definite matrices, respectively. \mathbb{RL}_∞ is the set of rational functions with real coefficients and no poles on the unit circle. $\mathbb{RH}_\infty \subset \mathbb{RL}_\infty$ contains functions that are analytic in the closed exterior of the unit disk in the complex plane. $\ell_2^{n_x}$ is the set of sequences $x : \mathbb{N} \rightarrow \mathbb{R}^{n_x}$ with $\|x\|_2 := \sqrt{\sum_{k=0}^{\infty} x(k)^\top x(k)} < \infty$. If $v, w \in \mathbb{R}^n$ then the inequality $v \leq w$ is element-wise, i.e. $v_i \leq w_i$ for $i = 1, \dots, n$. Similarly, $v \geq w$ is an elementwise inequality. For $P \in \mathbb{S}_{++}^n$, $x_* \in \mathbb{R}^n$, define the ellipsoid

$$\mathcal{E}(P, x_*) := \{x \in \mathbb{R}^n : (x - x_*)^\top P (x - x_*) \leq 1\}. \quad (1)$$

II. NOMINAL STABILITY ANALYSIS

A. Problem Formulation

Consider the feedback system consisting of a plant G and state-feedback controller π as shown in Figure 1. As a first

arXiv:2006.07579v1 [eess.SY] 13 Jun 2020

Funded in part by the Air Force Office of Scientific Research grant FA9550-18-1-0253, the Office of Naval Research grant N00014-18-1-2209, and the U.S. National Science Foundation grant ECCS-1906164.

H. Yin and M. Arcak are with the University of California, Berkeley {he_yin, arcak}@berkeley.edu.

P. Seiler is with the University of Michigan, Ann Arbor pseiler@umich.edu.

step, we assume the plant G is a linear, time-invariant (LTI) system defined by the following discrete-time model:

$$x(k+1) = A_G x(k) + B_G u(k), \quad (2)$$

where $x(k) \in \mathbb{R}^{n_G}$ is the state, $u(k) \in \mathbb{R}^{n_u}$ is the input, $A_G \in \mathbb{R}^{n_G \times n_G}$ and $B_G \in \mathbb{R}^{n_G \times n_u}$. The controller $\pi : \mathbb{R}^{n_G} \rightarrow \mathbb{R}^{n_u}$ is an ℓ -layer, feed-forward neural network (NN) defined as:

$$w^0(k) = x(k), \quad (3a)$$

$$w^i(k) = \phi^i (W^i w^{i-1}(k) + b^i), \quad i = 1, \dots, \ell, \quad (3b)$$

$$u(k) = W^{\ell+1} w^\ell(k) + b^{\ell+1}, \quad (3c)$$

where $w^i \in \mathbb{R}^{n_i}$ are the outputs (activations) from the i^{th} layer and $n_0 = n_G$. The operations for each layer are defined by a weight matrix $W^i \in \mathbb{R}^{n_i \times n_{i-1}}$, bias vector $b^i \in \mathbb{R}^{n_i}$, and activation function $\phi^i : \mathbb{R}^{n_i} \rightarrow \mathbb{R}^{n_i}$. The activation function ϕ^i is applied element-wise, i.e.

$$\phi^i(v) := [\varphi(v_1), \dots, \varphi(v_{n_i})]^\top, \quad (4)$$

where $\varphi : \mathbb{R} \rightarrow \mathbb{R}$ is the (scalar) activation function selected for the NN. Common choices for the scalar activation function include $\varphi(v) := \tanh(v)$, sigmoid $\varphi(v) := \frac{1}{1+e^{-v}}$, ReLU $\varphi(v) := \max(0, v)$, and leaky ReLU $\varphi(v) := \max(av, v)$ with $a \in (0, 1)$. We assume the activation φ is identical in all layers; this can be relaxed with minor changes to the notation.

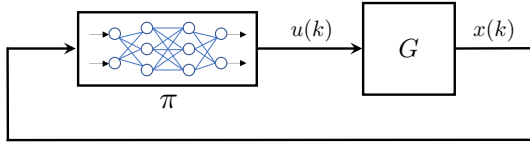


Fig. 1: Feedback system with plant G and NN π

The state vector x_* is an equilibrium point of the feedback system with input u_* if the following conditions hold:

$$x_* = A_G x_* + B_G u_*, \quad (5a)$$

$$u_* = \pi(x_*). \quad (5b)$$

Let $\chi(k; x_0)$ denote the solution to the feedback system at time k from initial condition $x(0) = x_0$. Our goal is to analyze asymptotic stability of the equilibrium point and to find the largest estimate of the region of attraction, defined below, using an ellipsoidal inner approximation.

Definition 1. The region of attraction (ROA) of the feedback system with plant G and NN π is defined as

$$\mathcal{R} := \{x_0 \in \mathbb{R}^{n_G} : \lim_{k \rightarrow \infty} \chi(k; x_0) = x_*\}. \quad (6)$$

B. NN Representation: Isolation of Nonlinearities

It is useful to isolate the nonlinear activation functions from the linear operations of the NN as done in [9], [17]. Define v^i as the input to the activation function ϕ^i :

$$v^i(k) := W^i w^{i-1}(k) + b^i, \quad i = 1, \dots, \ell. \quad (7)$$

The nonlinear operation of the i^{th} layer (Equation 3b) is thus expressed as $w^i(k) = \phi^i(v^i(k))$. Gather the inputs and outputs of all activation functions:

$$v_\phi := \begin{bmatrix} v^1 \\ \vdots \\ v^\ell \end{bmatrix} \in \mathbb{R}^{n_\phi} \quad \text{and} \quad w_\phi := \begin{bmatrix} w^1 \\ \vdots \\ w^\ell \end{bmatrix} \in \mathbb{R}^{n_\phi}, \quad (8)$$

where $n_\phi := n_1 + \dots + n_\ell$, and define the combined nonlinearity $\phi : \mathbb{R}^{n_\phi} \rightarrow \mathbb{R}^{n_\phi}$ by stacking the activation functions:

$$\phi(v_\phi) := \begin{bmatrix} \phi^1(v^1) \\ \vdots \\ \phi^\ell(v^\ell) \end{bmatrix}. \quad (9)$$

Thus $w_\phi(k) = \phi(v_\phi(k))$, where the scalar activation function φ is applied element-wise to each entry of v_ϕ . Finally, the NN control policy π defined in Equation 3 can be rewritten as:

$$\begin{bmatrix} u(k) \\ v_\phi(k) \end{bmatrix} = N \begin{bmatrix} x(k) \\ w_\phi(k) \\ 1 \end{bmatrix} \quad (10a)$$

$$w_\phi(k) = \phi(v_\phi(k)). \quad (10b)$$

The matrix N depends on the weights and biases as follows, where the vertical and horizontal bars partition N compatibly with the inputs $(x, w_\phi, 1)$ and outputs (u, v_ϕ) :

$$N := \begin{bmatrix} 0 & 0 & 0 & \dots & W^{\ell+1} & b^{\ell+1} \\ \hline W^1 & 0 & \dots & 0 & 0 & b^1 \\ 0 & W^2 & \dots & 0 & 0 & b^2 \\ \vdots & \vdots & \ddots & \vdots & \vdots & \vdots \\ 0 & 0 & \dots & W^\ell & 0 & b^\ell \end{bmatrix} \quad (11a)$$

$$:= \begin{bmatrix} N_{ux} & N_{uw} & N_{ub} \\ N_{vx} & N_{vw} & N_{vb} \end{bmatrix}. \quad (11b)$$

This decomposition of the NN, depicted in Figure 2, isolates the activation functions in preparation for the stability analysis.

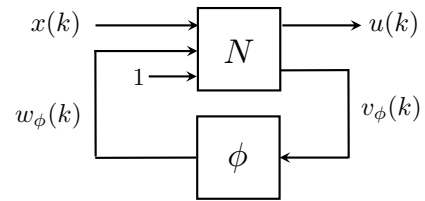


Fig. 2: NN representation to isolate the nonlinearities ϕ .

Suppose (x_*, u_*) satisfies Equation 5. Then x_* can be propagated through the NN to obtain equilibrium values v_*^i, w_*^i for the inputs/outputs of each activation function ($i = 1, \dots, \ell$), yielding $(v_\phi, w_\phi) = (v_*, w_*)$. Thus (x_*, u_*, v_*, w_*) is an equilibrium point of (2) and (3) if:

$$x_* = A_G x_* + B_G u_*, \quad (12a)$$

$$\begin{bmatrix} u_* \\ v_* \end{bmatrix} = N \begin{bmatrix} x_* \\ w_* \\ 1 \end{bmatrix}, \quad (12b)$$

$$w_* = \phi(v_*). \quad (12c)$$

C. Quadratic Constraints: Scalar Activation Functions

The stability analysis relies on quadratic constraints to bound the activation function. A typical constraint is the sector bound as defined next.

Definition 2. Let $\alpha \leq \beta$ be given. The function $\varphi : \mathbb{R} \rightarrow \mathbb{R}$ lies in the (global) sector $[\alpha, \beta]$ if:

$$(\varphi(\nu) - \alpha\nu) \cdot (\beta\nu - \varphi(\nu)) \geq 0 \quad \forall \nu \in \mathbb{R}. \quad (13)$$

The interpretation of the sector $[\alpha, \beta]$ is that φ lies between lines passing through the origin with slope α and β . Many activation functions are bounded in the sector $[0, 1]$, e.g. \tanh and ReLU. Figure 3 illustrates $\varphi(\nu) = \tanh(\nu)$ (blue solid) and the global sector defined by $[0, 1]$ (red solid lines).

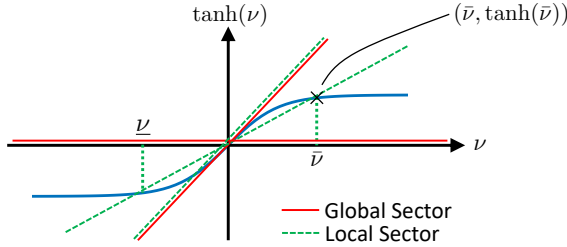


Fig. 3: Sector constraints on tanh

The global sector constraint is often too coarse for stability analysis, and a local sector constraint provides tighter bounds.

Definition 3. Let $\alpha, \beta, \underline{\nu}, \bar{\nu} \in \mathbb{R}$ with $\alpha \leq \beta$ and $\underline{\nu} \leq 0 \leq \bar{\nu}$. The function $\varphi : \mathbb{R} \rightarrow \mathbb{R}$ satisfies the local sector $[\alpha, \beta]$ if

$$(\varphi(\nu) - \alpha\nu) \cdot (\beta\nu - \varphi(\nu)) \geq 0 \quad \forall \nu \in [\underline{\nu}, \bar{\nu}]. \quad (14)$$

As an example, $\varphi(\nu) := \tanh(\nu)$ restricted to the interval $[-\bar{\nu}, \bar{\nu}]$ satisfies the local sector bound $[\alpha, \beta]$ with $\alpha := \tanh(\bar{\nu})/\bar{\nu} > 0$ and $\beta := 1$. As shown in Figure 3 (green dashed lines), the local sector provides a tighter bound than the global sector. These bounds are valid for a symmetric interval around the origin with $\underline{\nu} = -\bar{\nu}$; non-symmetric intervals ($\underline{\nu} \neq -\bar{\nu}$) can be handled similarly.

The local and global sector constraints above were defined to be centered at the point $(\nu, \varphi(\nu)) = (0, 0)$. The stability analysis will require offset sectors centered around an arbitrary point $(\nu_*, \varphi(\nu_*))$ on the function. For example, $\varphi(\nu) = \tanh(\nu)$ satisfies the global sector bound (red solid) around the point $(\nu_*, \tanh(\nu_*))$ with $[\alpha, \beta] = [0, 1]$, as shown in Figure 4. It satisfies a tighter local sector bound (green dashed) when the input is restricted to $\nu \in [\underline{\nu}, \bar{\nu}]$. An explicit expression for this local sector is $\beta = 1$ and

$$\alpha := \min \left(\frac{\tanh(\bar{\nu}) - \tanh(\nu_*)}{\bar{\nu} - \nu_*}, \frac{\tanh(\nu_*) - \tanh(\underline{\nu})}{\nu_* - \underline{\nu}} \right).$$

The local sector upper bound β can be tightened further. This leads to the following definition of an offset local sector.

Definition 4. Let $\alpha, \beta, \underline{\nu}, \bar{\nu}, \nu_* \in \mathbb{R}$ be given with $\alpha \leq \beta$ and $\underline{\nu} \leq \nu_* \leq \bar{\nu}$. The function $\varphi : \mathbb{R} \rightarrow \mathbb{R}$ satisfies the offset local sector $[\alpha, \beta]$ around the point ν_* if:

$$(\Delta\varphi(\nu) - \alpha\Delta\nu) \cdot (\beta\Delta\nu - \Delta\varphi(\nu)) \geq 0 \quad \forall \nu \in [\underline{\nu}, \bar{\nu}] \quad (15)$$

where $\Delta\varphi(\nu) := \varphi(\nu) - \varphi(\nu_*)$ and $\Delta\nu := \nu - \nu_*$.

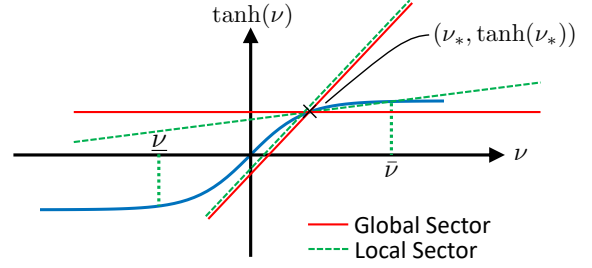


Fig. 4: Offset local sector constraint on tanh

D. Quadratic Constraints: Combined Activation Functions

Offset local sector constraints can also be defined for the combined nonlinearity ϕ , given by Equation 9. Let $\underline{v}, \bar{v}, v_* \in \mathbb{R}^{n_\phi}$ be given with $\underline{v} \leq v_* \leq \bar{v}$. Assume that the activation input $v_\phi \in \mathbb{R}^{n_\phi}$ lies, element-wise, in the interval $[\underline{v}, \bar{v}]$ and the i^{th} input/output pair is $w_i = \phi(v_i)$. Further assume the scalar activation function satisfies the local sector $[\alpha_i, \beta_i]$ around the point $v_{*,i}$ with the input restricted to $v_i \in [\underline{v}_i, \bar{v}_i]$ for $i = 1, \dots, n_\phi$. The local sector bounds can be computed for φ on the given interval either analytically (as above for \tanh) or numerically. These local sectors can be stacked into vectors $\alpha_\phi, \beta_\phi \in \mathbb{R}^{n_\phi}$ that provide quadratic constraints satisfied by the combined nonlinearity ϕ .

Lemma 1. Let $\alpha_\phi, \beta_\phi, \underline{v}, \bar{v}, v_* \in \mathbb{R}^{n_\phi}$ be given with $\alpha_\phi \leq \beta_\phi$, $\underline{v} \leq v_* \leq \bar{v}$, and $w_* := \phi(v_*)$. Assume ϕ satisfies the offset local sector $[\alpha_\phi, \beta_\phi]$ around the point v_* element-wise for all $v_\phi \in [\underline{v}, \bar{v}]$. If $\lambda \in \mathbb{R}^{n_\phi}$ with $\lambda \geq 0$ then:

$$\begin{bmatrix} v_\phi - v_* \\ w_\phi - w_* \end{bmatrix}^\top \Psi_\phi^\top M_\phi(\lambda) \Psi_\phi \begin{bmatrix} v_\phi - v_* \\ w_\phi - w_* \end{bmatrix} \geq 0$$

$$\forall v_\phi \in [\underline{v}, \bar{v}], w_\phi = \phi(v_\phi),$$

where:

$$\Psi_\phi := \begin{bmatrix} \text{diag}(\beta_\phi) & -I_{n_\phi} \\ -\text{diag}(\alpha_\phi) & I_{n_\phi} \end{bmatrix} \quad (16)$$

$$M_\phi(\lambda) := \begin{bmatrix} 0_{n_\phi} & \text{diag}(\lambda) \\ \text{diag}(\lambda) & 0_{n_\phi} \end{bmatrix}. \quad (17)$$

Proof. For any $v_\phi \in \mathbb{R}^{n_\phi}$ and $w_\phi = \phi(v_\phi)$:

$$\begin{bmatrix} v_\phi - v_* \\ w_\phi - w_* \end{bmatrix}^\top \Psi_\phi^\top M_\phi(\lambda) \Psi_\phi \begin{bmatrix} v_\phi - v_* \\ w_\phi - w_* \end{bmatrix}$$

$$= \sum_{i=1}^{n_\phi} \lambda_i (\Delta w_i - \alpha \Delta v_i) \cdot (\beta \Delta v_i - \Delta w_i)$$

where $\Delta w_i := \phi(v_i) - \phi(v_{*,i})$ and $\Delta v_i := v_i - v_{*,i}$. If $v_\phi \in [\underline{v}, \bar{v}]$ then each term in the sum is non-negative by the offset local sector constraints and $\lambda \geq 0$. \square

The stability theorem in the next section must verify that $v \in [\underline{v}, \bar{v}]$ in order to apply the sector bounds. The analysis is simplified by constructing the sector bounds based only on the input to the first activation layer. Specifically, let v_*^1 be the equilibrium value at the first NN layer. Select $\underline{v}^1, \bar{v}^1 \in \mathbb{R}^{n_1}$ with $\underline{v}^1 \leq v_*^1 \leq \bar{v}^1$. The assumed bounds $[\underline{v}^1, \bar{v}^1]$ can be used to compute a local sector $[\alpha^1, \beta^1]$ around the point v_*^1

for the first activation function ϕ^1 , i.e. the i^{th} input/output pair of ϕ^1 is locally sector bounded by $[\alpha_i^1, \beta_i^1]$. The bounds on v^1 can also be used to compute an interval $[\underline{w}^1, \bar{w}^1]$ for the output $w^1 = \phi^1(v^1)^\dagger$ which can then be used to compute bounds $[\underline{v}^2, \bar{v}^2]$ on the input v^2 to the next activation function.[‡] The intervals computed for w^1 and v^2 will contain their equilibrium value w_*^1 and v_*^2 . This process can be propagated through all layers of the NN to obtain local sector bounds $[\alpha^i, \beta^i]$ for the nonlinearities ϕ^i ($i = 1, \dots, \ell$). The sectors can be stacked into vectors $\alpha_\phi, \beta_\phi \in \mathbb{R}^{n_\phi}$ that provide (element-wise) local sector bounds as summarized next.

Property 1. Let $v_* \in \mathbb{R}^{n_\phi}$ be an equilibrium value of the activation input and $v_*^1 \in \mathbb{R}^{n_1}$ be the corresponding value at the first layer. Select $\underline{v}^1, \bar{v}^1 \in \mathbb{R}^{n_1}$ with $v_*^1 \in [\underline{v}^1, \bar{v}^1]$. Let $\hat{v}_\phi(v^1) \in \mathbb{R}^{n_\phi}$ denote the activation input generated by the NN (Equation 3b) from the input $v^1 \in \mathbb{R}^{n_1}$ at the first layer. There exist $\alpha_\phi, \beta_\phi \in \mathbb{R}^{n_\phi}$ such that ϕ satisfies the offset local sector around the point $(v_*, \phi(v_*))$ for all $\hat{v}_\phi(v^1)$ with $v^1 \in [\underline{v}^1, \bar{v}^1]$.

E. Lyapunov Condition

This section uses a Lyapunov function and the offset local sector to compute an inner approximation for the ROA of the feedback system of G and π . To simplify notation, the interval bound on v^1 is assumed to be symmetrical about v_*^1 , i.e. $\underline{v}^1 = 2v_*^1 - \bar{v}^1$ so that $\bar{v}^1 - v_*^1 = v_*^1 - \underline{v}^1$. This can be relaxed to handle non-symmetrical intervals with minor notational changes.

Theorem 1. Consider the feedback system of plant G in (2) and NN π in (3) with equilibrium point (x_*, u_*, v_*, w_*) satisfying (12). Let $\bar{v}^1 \in \mathbb{R}^{n_1}$, $\underline{v}^1 := 2v_*^1 - \bar{v}^1$, and $\alpha_\phi, \beta_\phi \in \mathbb{R}^{n_\phi}$ be given vectors satisfying Property 1 for the NN. Denote the i^{th} row of the first weight W^1 by W_i^1 and define matrices

$$R_V := \begin{bmatrix} I_{n_G} & 0_{n_G \times n_\phi} \\ N_{ux} & N_{uw} \end{bmatrix}, \text{ and } R_\phi := \begin{bmatrix} N_{vx} & N_{vw} \\ 0_{n_\phi \times n_G} & I_{n_\phi} \end{bmatrix}.$$

If there exists a matrix $P \in \mathbb{S}_{+++}^{n_G}$, and vector $\lambda \in \mathbb{R}^{n_\phi}$ with $\lambda \geq 0$ such that

$$R_V^\top \begin{bmatrix} A_G^\top P A_G - P & A_G^\top P B_G \\ B_G^\top P A_G & B_G^\top P B_G \end{bmatrix} R_V + R_\phi^\top \Psi_\phi^\top M_\phi(\lambda) \Psi_\phi R_\phi < 0, \quad (20)$$

$$\begin{bmatrix} (\bar{v}_i^1 - v_{*,i}^1)^2 & W_i^1 \\ W_i^{1\top} & P \end{bmatrix} \geq 0, \quad i = 1, \dots, n_1, \quad (21)$$

[†]For example, if $\varphi(\nu) = \tanh(\nu)$ then the input bound $\nu \in [-\bar{\nu}, \bar{\nu}]$ implies the output bound $\varphi(\nu) \in [-\tanh(\bar{\nu}), \tanh(\bar{\nu})]$.

[‡]The next activation input is $v^2 := W^2 w^1 + b^2$. The largest value of the i^{th} entry of this vector is obtained by solving the following optimization:

$$\bar{v}_i^2 := \max_{\underline{w}^1 \leq w^1 \leq \bar{w}^1} y^\top w^1 + b_i^2 \quad (18)$$

where y^\top is the i^{th} row of W^2 . Define $c := \frac{1}{2}(\bar{w}^1 + \underline{w}^1)$ and $r := \frac{1}{2}(\bar{w}^1 - \underline{w}^1)$. The optimization can be rewritten as:

$$\bar{v}_i^2 := \left(y^\top c + b_i^2 \right) + \max_{-r \leq \delta \leq r} y^\top \delta \quad (19)$$

This has the explicit solution $\bar{v}_i^2 = y^\top c + b_i^2 + \sum_{j=1}^{n_1} |y_j r_j|$. Similarly, the minimal value is $\underline{v}_i^2 = y^\top c + b_i^2 - \sum_{j=1}^{n_1} |y_j r_j|$.

then: (i) the feedback system consisting of G and π is locally stable around x_* , and (ii) the set $\mathcal{E}(P, x_*)$, defined by Equation 1, is an inner-approximation to the ROA.

Proof. By Schur complements, (21) is equivalent to:

$$W_i^1 P^{-1} W_i^{1\top} \leq (\bar{v}_i^1 - v_{*,i}^1)^2, \quad i = 1, \dots, n_1. \quad (22)$$

It follows from Lemma 1 in [20] that:

$$\mathcal{E}(P, x_*) \subseteq \{x \in \mathbb{R}^{n_G} : \underline{v}^1 - v_*^1 \leq W^1(x - x_*) \leq \bar{v}^1 - v_*^1\}.$$

Finally, use $v^1 - v_*^1 = W^1(x - x_*)$ to rewrite this as:

$$\mathcal{E}(P, x_*) \subseteq \{x : \underline{v}^1 \leq v^1 \leq \bar{v}^1\}.$$

To summarize, feasibility of (21) verifies that if $x(k) \in \mathcal{E}(P, x_*)$ then $v^1(k) \in [\underline{v}^1, \bar{v}^1]$ and hence the offset local sectors conditions are valid.

Next, left / right multiply the LMI (20) by any (non-zero) $[(x(k) - x_*)^\top \quad (w_\phi(k) - w_*)^\top]$ and its transpose to obtain

$$\begin{bmatrix} x(k) - x_* \\ u(k) - u_* \end{bmatrix}^\top \begin{bmatrix} A_G^\top P A_G - P & A_G^\top P B_G \\ B_G^\top P A_G & B_G^\top P B_G \end{bmatrix} \begin{bmatrix} x(k) - x_* \\ u(k) - u_* \end{bmatrix} + \begin{bmatrix} v_\phi(k) - v_* \\ w_\phi(k) - w_* \end{bmatrix}^\top \Psi_\phi^\top M_\phi(\lambda) \Psi_\phi \begin{bmatrix} v_\phi(k) - v_* \\ w_\phi(k) - w_* \end{bmatrix} < 0.$$

Define the Lyapunov function $V(x) := (x - x_*)^\top P(x - x_*)$ and use (2) and (12) to show:

$$V(x(k+1)) - V(x(k)) + \begin{bmatrix} v_\phi(k) - v_* \\ w_\phi(k) - w_* \end{bmatrix}^\top \Psi_\phi^\top M_\phi(\lambda) \Psi_\phi \begin{bmatrix} v_\phi(k) - v_* \\ w_\phi(k) - w_* \end{bmatrix} < 0. \quad (23)$$

As noted above, $x(k) \in \mathcal{E}(P, x_*)$ implies the offset local sector $[\alpha_\phi, \beta_\phi]$ around v_* . Then, by Lemma 1, the final term in (23) is ≥ 0 and it follows from a Lyapunov argument, e.g. Theorem 4.1 in [7], that x_* is an asymptotically stable equilibrium point and $\mathcal{E}(P, x_*)$ is an inner approximation of the ROA. \square

This stability theorem can be made less conservative by incorporating global slope bounds on φ in addition to the local sector bounds. Slope bounds provide quadratic constraints between two inputs $\nu_1, \nu_2 \in \mathbb{R}$ and their corresponding outputs $\varphi(\nu_1), \varphi(\nu_2)$. These constraints can be exploited in two different ways. First, the slope bounds provide constraints that relate the activation at different time instances, e.g. between $\phi_i(v_{\phi,i}(k))$ and $\phi_i(v_{\phi,i}(k+1))$ for any $i = 1, \dots, n_\phi$. These temporal relations are captured by the Zames-Falb IQC [21], [22]. Second, it provides constraints that relate the scalar activation functions repeated in ϕ at the same time instant, e.g. between $\phi_i(v_{\phi,i}(k))$ and $\phi_j(v_{\phi,j}(k))$.

III. ROBUST STABILITY ANALYSIS

A. Problem Formulation

Consider the uncertain feedback system in Figure 5, consisting of an uncertain plant $F_u(G, \Delta)$ and a NN controller π as defined by (3). The uncertain plant $F_u(G, \Delta)$ is an interconnection of a nominal plant G and a perturbation Δ . The nominal plant G is defined by the following equations:

$$x(k+1) = A_G x(k) + B_{G1} q(k) + B_{G2} u(k), \quad (24a)$$

$$p(k) = C_G x(k) + D_{G1} q(k) + D_{G2} u(k), \quad (24b)$$

where $x(k) \in \mathbb{R}^{n_G}$ is the state, $u(k) \in \mathbb{R}^{n_u}$ is the control input, $p(k) \in \mathbb{R}^{n_p}$ and $q(k) \in \mathbb{R}^{n_q}$ are the input and output of Δ , $A_G \in \mathbb{R}^{n_G \times n_G}$, $B_{G1} \in \mathbb{R}^{n_G \times n_q}$, $B_{G2} \in \mathbb{R}^{n_G \times n_u}$, $C_G \in \mathbb{R}^{n_p \times n_G}$, $D_{G1} \in \mathbb{R}^{n_p \times n_q}$, and $D_{G2} \in \mathbb{R}^{n_p \times n_u}$. The perturbation is a bounded, causal operator $\Delta : \ell_{2e}^{n_p} \rightarrow \ell_{2e}^{n_q}$. The nominal plant G and perturbation Δ form the interconnection $F_u(G, \Delta)$ through the constraint

$$q(\cdot) = \Delta(p(\cdot)). \quad (25)$$

The vectors (x_*, u_*, p_*, q_*) form an equilibrium point of the feedback system if the following conditions hold:

$$x_* = A_G x_* + B_{G1} q_* + B_{G2} u_*, \quad (26a)$$

$$u_* = \pi(x_*), \quad (26b)$$

$$q_*^s = \Delta(p_*^s), \quad (26c)$$

where Equation 26c states that the constant input $p_*^s := \{p_*, p_*, \dots\}$ maps to the constant output $q_*^s := \{q_*, q_*, \dots\}$. Note that Δ is modeled as an operator mapping inputs to outputs. If Δ has an internal state then there is an implicit assumption that its initial condition is such that $q_*^s = \Delta(p_*^s)$.

Let $\chi(k; x_0)$ denote the solution to the uncertain feedback system at time k from the initial condition $x(0) = x_0$.[§] Define the robust ROA associated with x_* as follows.

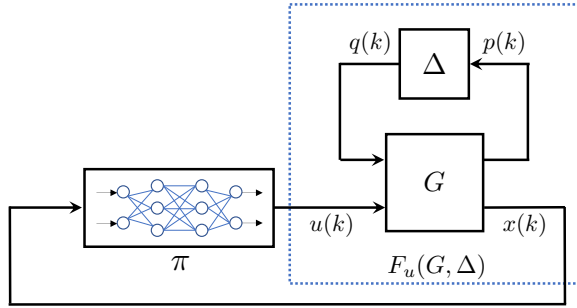


Fig. 5: Feedback system with uncertain plant $F_u(G, \Delta)$ and NN controller π

Definition 5. The robust ROA of the feedback system with the uncertain plant $F_u(G, \Delta)$ and NN π is defined as:

$$\mathcal{R} := \{x_0 \in \mathbb{R}^{n_G} : \lim_{k \rightarrow \infty} \chi(k; x_0) = x_*\}. \quad (27)$$

The objective is to prove the uncertain feedback system is asymptotically stable and, if so, to find the largest estimate of the robust ROA using an ellipsoidal inner approximation.

B. Integral Quadratic Constraints

The perturbation can represent various types of uncertainty [18], [19], including saturation, time delay, unmodeled dynamics, and slope-restricted nonlinearities. The input-output relationship of Δ is characterized with an integral quadratic constraint (IQC), which consists of a ‘virtual’ filter Ψ_Δ applied

[§]An input/output model is used for the perturbation Δ so that its internal state and initial condition is not explicitly considered.

to the input p and output q of Δ and a constraint on the output r of Ψ_Δ . The filter Ψ_Δ is an LTI system of the form:

$$\psi(k+1) = A_\Psi \psi(k) + B_{\Psi1} p(k) + B_{\Psi2} q(k) \quad (28a)$$

$$r(k) = C_\Psi \psi(k) + D_{\Psi1} p(k) + D_{\Psi2} q(k). \quad (28b)$$

$$\psi(0) = \psi_* \quad (28c)$$

where $\psi(k) \in \mathbb{R}^{n_\psi}$ is the state and $r(k) \in \mathbb{R}^{n_r}$ is the output. The state matrices have compatible dimensions. The vectors $\psi_* \in \mathbb{R}^{n_\psi}$ and $r_* \in \mathbb{R}^{n_r}$ are equilibrium states and output of (28) with inputs p_* and q_* such that Equation 26c holds, i.e.,

$$\psi_* = A_\Psi \psi_* + B_{\Psi1} p_* + B_{\Psi2} q_* \quad (29a)$$

$$r_* = C_\Psi \psi_* + D_{\Psi1} p_* + D_{\Psi2} q_*. \quad (29b)$$

The Lyapunov analysis in the next subsection makes use of time-domain IQCs as defined next:

Definition 6. Let $\Psi_\Delta \in \mathbb{RH}_\infty^{n_r \times (n_p + n_q)}$ and $M_\Delta \in \mathbb{S}^{n_r}$ be given. A bounded, causal operator $\Delta : \ell_{2e}^{n_p} \rightarrow \ell_{2e}^{n_q}$ satisfies the time domain IQC defined by (Ψ_Δ, M_Δ) if the following inequality holds for all $p \in \ell_{2e}^{n_p}$, $q = \Delta(p)$ and for all $N \geq 0$

$$\sum_{k=0}^N (r(k) - r_*)^\top M_\Delta (r(k) - r_*) \geq 0. \quad (30)$$

where $r(k)$ and r_* are defined by (28b) and (29b).

The notation $\Delta \in \text{IQC}(\Psi_\Delta, M_\Delta)$ indicates that Δ satisfies the IQC defined by Ψ_Δ and M_Δ . Therefore, the precise relation (25), for analysis, is replaced by the constraint (30) on r . The quadratic constraint proposed in Lemma 1 is a special instance of a time-domain IQCs. Specifically, Lemma 1 defines a quadratic constraints that holds at each time step k and hence the inequality also holds summing over any finite horizons. This is referred to as the offset local sector IQC.

The time-domain IQCs, as defined here, hold on any finite horizon $N \geq 0$. These are typically called ‘hard IQCs’ [18]. IQCs can also be defined in the frequency domain and equivalently expressed as time-domain constraints over an infinite horizon ($N = \infty$). These are called soft IQCs. Although this paper focuses on the use of hard IQCs, it is possible to also incorporate soft IQCs [23]–[25].

C. Lyapunov Condition

Let $\zeta := \begin{bmatrix} x \\ \psi \end{bmatrix} \in \mathbb{R}^{n_\zeta}$ define the extended state vector, $n_\zeta = n_G + n_\psi$, whose dynamics are

$$\zeta(k+1) = \mathcal{A} \zeta(k) + \mathcal{B} \begin{bmatrix} q(k) \\ u(k) \end{bmatrix} \quad (31a)$$

$$r(k) = \mathcal{C} \zeta(k) + \mathcal{D} \begin{bmatrix} q(k) \\ u(k) \end{bmatrix} \quad (31b)$$

$$u(k) = \pi(x(k)) \quad (31c)$$

where the state-space matrices are

$$\mathcal{A} = \begin{bmatrix} A_G & 0 \\ B_{\Psi1} C_G & A_\Psi \end{bmatrix}, \quad \mathcal{B} = \begin{bmatrix} B_{G1} & B_{G2} \\ B_{\Psi1} D_{G1} + B_{\Psi2} & B_{\Psi1} D_{G2} \end{bmatrix},$$

$$\mathcal{C} = \begin{bmatrix} D_{\Psi1} C_G & C_\Psi \end{bmatrix}, \quad \mathcal{D} = \begin{bmatrix} D_{\Psi1} D_{G1} + D_{\Psi2} & D_{\Psi1} D_{G2} \end{bmatrix}.$$

Let $\zeta_* := \begin{bmatrix} x_* \\ \psi_* \end{bmatrix}$ define the equilibrium point of the extended system (31). Since IQCs implicitly constrain the input p of the extended system (31), the response of the extended system subject to IQCs “covers” the behaviors of the original uncertain feedback system. The following theorem provides a method for inner-approximating the robust ROA by performing analysis on the extended system subject to IQCs.

Theorem 2. *Consider the feedback system of an uncertain plant $F_u(G, \Delta)$ in (24)–(25), and the NN π in (3) with equilibrium point $(\zeta_*, u_*, v_*, w_*, r_*, p_*, q_*)$ satisfying (26) and (29). Assume $\Delta \in \text{IQC}(\Psi_\Delta, M_\Delta)$ with Ψ_Δ and M_Δ given. Let $\bar{v}^1 \in \mathbb{R}^{n_1}$, $v^1 := 2v_*^1 - \bar{v}^1$, and $\alpha_\phi, \beta_\phi \in \mathbb{R}^{n_\phi}$ be given vectors satisfying Property 1 for the NN, and define matrices*

$$R_V = \begin{bmatrix} I_{n_\zeta} & 0 & 0 \\ 0 & 0 & I_{n_q} \\ N_{u\zeta} & N_{uw} & 0 \end{bmatrix}, \quad N_{u\zeta} = [N_{ux}, 0_{n_u \times n_\psi}],$$

$$R_\phi = \begin{bmatrix} N_{v\zeta} & N_{vw} & 0 \\ 0 & I_{n_\phi} & 0 \end{bmatrix}, \quad N_{v\zeta} = [N_{vx}, 0_{n_\phi \times n_\psi}],$$

$$\mathcal{W}_i^1 = [W_i^1 \quad 0_{1 \times n_\psi}], \quad W_i^1 \text{ is the } i^{\text{th}} \text{ row of } W^1.$$

If there exists a matrix $P \in \mathbb{S}_{++}^{n_\zeta}$, and vector $\lambda \in \mathbb{R}^{n_\phi}$ with $\lambda \geq 0$ such that

$$R_V^\top \begin{bmatrix} \mathcal{A}^\top P \mathcal{A} - P & \mathcal{A}^\top P \mathcal{B} \\ \mathcal{B}^\top P \mathcal{A} & \mathcal{B}^\top P \mathcal{B} \end{bmatrix} R_V + R_\phi^\top \Psi_\Phi^\top M_\phi(\lambda) \Psi_\phi R_\phi + R_V^\top [\mathcal{C} \quad \mathcal{D}]^\top M_\Delta [\mathcal{C} \quad \mathcal{D}] R_V < 0, \quad (32a)$$

$$\begin{bmatrix} (\bar{v}_i^1 - v_{*,i}^1)^2 & W_i^1 \\ \mathcal{W}_i^{1\top} & P \end{bmatrix} \geq 0, \quad i = 1, \dots, n_1, \quad (32b)$$

then: (i) the feedback system comprising the uncertain plant $F_u(G, \Delta)$ and π is locally stable around x_* for any $\Delta \in \text{IQC}(\Psi_\Delta, M_\Delta)$, and (ii) the intersection of $\mathcal{E}(P, \zeta_*)$ with the hyperplane $\psi = \psi_*$, i.e. $\mathcal{E}(P_x, x_*)$ where $P_x \in \mathbb{R}^{n_G \times n_G}$ is the upper left block of P , is an inner-approximation to the robust ROA.

Proof. As in the proof of Theorem 1, feasibility of (32b) implies that if $\zeta(k) \in \mathcal{E}(P, \zeta_*)$ then $v^1(k) \in [v^1, \bar{v}^1]$ and hence the offset local sectors conditions are valid. Since the LMI in (32a) is strict, there exists $\epsilon > 0$ such that left/right multiplication of the LMI by $[(\zeta(k) - \zeta_*)^\top, (w_\phi(k) - w_*)^\top, (q(k) - q_*)^\top]$ and its transpose yields:

$$\begin{aligned} & \begin{bmatrix} \star \\ \star \\ \star \end{bmatrix}^\top \begin{bmatrix} \mathcal{A}^\top P \mathcal{A} - P & \mathcal{A}^\top P \mathcal{B} \\ \mathcal{B}^\top P \mathcal{A} & \mathcal{B}^\top P \mathcal{B} \end{bmatrix} \begin{bmatrix} \zeta(k) - \zeta_* \\ q(k) - q_* \\ u(k) - u_* \end{bmatrix} \\ & + \begin{bmatrix} \star \\ \star \end{bmatrix}^\top [\mathcal{C} \quad \mathcal{D}]^\top M_\Delta [\mathcal{C} \quad \mathcal{D}] \begin{bmatrix} \zeta(k) - \zeta_* \\ q(k) - q_* \\ u(k) - u_* \end{bmatrix} \\ & + \begin{bmatrix} \star \\ \star \end{bmatrix}^\top \Psi_\phi^\top M_\phi(\lambda) \Psi_\phi \begin{bmatrix} v_\phi(k) - v_* \\ w_\phi(k) - w_* \end{bmatrix} \leq -\epsilon \|\zeta(k) - \zeta_*\|^2, \end{aligned}$$

where the entries denoted by \star can be inferred from symmetry. Define the Lyapunov function $V(\zeta) := (\zeta - \zeta_*)^\top P (\zeta - \zeta_*)$, and use (26), (29) and (31) to show:

$$\begin{aligned} & V(\zeta(k+1)) - V(\zeta(k)) + (r(k) - r_*)^\top M_\Delta (r(k) - r_*) \\ & + \begin{bmatrix} \star \\ \star \end{bmatrix}^\top \Psi_\phi^\top M_\phi(\lambda) \Psi_\phi \begin{bmatrix} v_\phi(k) - v_* \\ w_\phi(k) - w_* \end{bmatrix} \leq -\epsilon \|\zeta(k) - \zeta_*\|^2. \end{aligned}$$

Sum this inequality from $k = 0$ to any finite time $N \geq 0$. The third and fourth term on the left side will be ≥ 0 by the local sector conditions and the IQC. This yields:

$$V(\zeta(N+1)) - V(\zeta(0)) \leq -\sum_{k=0}^N \epsilon \|\zeta(k) - \zeta_*\|^2.$$

Thus if $\zeta(0) \in \mathcal{E}(P, \zeta_*)$ then $\zeta(k) \in \mathcal{E}(P, \zeta_*)$ for all $k \geq 0$. Moreover, this inequality implies that $\zeta(N) \rightarrow \zeta_*$ as $N \rightarrow \infty$. The initial condition for the virtual filter is $\psi(0) = \psi_*$ so that $\zeta(0) \in \mathcal{E}(P, \zeta_*)$ is equivalent to $x(0) \in \mathcal{E}(P_x, x_*)$. Hence $\mathcal{E}(P_x, x_*)$ is an inner approximation for the ROA. \square

For a particular perturbation Δ there is typically a class of valid time-domain IQCs defined by a fixed filter Ψ_Δ and a matrix M_Δ drawn from a constraint set \mathcal{M}_Δ . Therefore when formulating an optimization problem, along with P and λ , we can treat $M_\Delta \in \mathcal{M}_\Delta$ as an additional decision variable to reduce conservatism. In this paper, the set \mathcal{M}_Δ is restricted to one that is described by LMIs [19]. The “largest” inner-approximation to the ROA can be obtained by minimizing $\text{trace}(P_x)$ or some other metric related to the ellipsoid volume.

IV. EXAMPLES

A. Inverted pendulum

Consider the nonlinear inverted pendulum example from [26] with mass $m = 0.15$ kg, length $l = 0.5$ m, and friction coefficient $\mu = 0.5$ Nms/rad. The dynamics are:

$$\ddot{\theta}(t) = \frac{mgl \sin(\theta(t)) - \mu \dot{\theta}(t) + u(t)}{ml^2}, \quad (33)$$

where θ is the angular position (rad) and u is the control input (Nm). The plant state is $x = [\theta, \dot{\theta}]$. The controller π is obtained through a reinforcement learning process using policy gradient [3]–[5]. During training, the agent decision making process is characterized by a probability: $u(k) \sim Pr(u(k) = u \mid x(k) = x)$ for all $u \in \mathbb{R}$ and $x \in \mathbb{R}^2$ where the probability is a Gaussian distribution with mean $\pi(x(k))$, and standard deviation σ . After training, the policy mean π is used as the deterministic controller $u(k) = \pi(x(k))$. The controller π is parameterized by a 2-layer, feedforward NN with $n_1 = n_2 = 32$ and tanh as the activation function for both layers. The biases in the NN are set to zero during training to ensure that the equilibrium point is $x_* = 0$ and $u_* = 0$. The dynamics used for training are the discretized version of (33) with sampling time $dt = 0.02$ s.

The system (33) is nonlinear due to the trigonometric term $\sin(\theta)$. The robust ROA analysis framework can be applied by rearranging (33) into the form:

$$\ddot{\theta}(t) = \frac{-mglq(t) + mgl\theta(t) - \mu\dot{\theta}(t) + u(t)}{ml^2}, \quad (34a)$$

$$q(t) = \Delta(\theta(t)) := \theta(t) - \sin(\theta(t)). \quad (34b)$$

The static nonlinearity $\Delta(\theta) = \theta - \sin(\theta)$, treated as a perturbation, is slope-restricted in the interval $[0, 2]$, and sector bounded in the sector $[0, 1]$ for $\theta \in [-3.14, 3.14]$ as shown in Figure 6. Local slope and sector bounds can be derived to provide less conservative results on shorter intervals $[\underline{\theta}, \bar{\theta}]$.

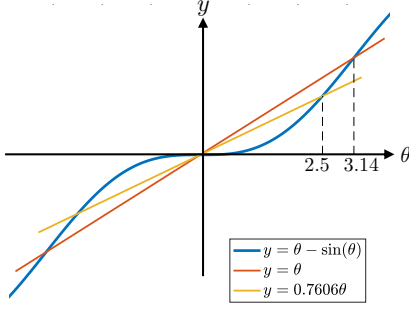


Fig. 6: Local sector bounds for Δ

For example, if $\bar{\theta} = -\underline{\theta} = 2.5$ then the nonlinearity is slope-restricted in $[0, 1.8]$, and sector bounded in $[0, 0.7606]$. This local sector is shown in Fig. 6. In this example, it is assumed that $v^1 \in [\underline{v}^1, \bar{v}^1]$ with $\bar{v}^1 = -v^1 = 0.5 \times 1_{32 \times 1}$. It is also assumed that $\theta(k) \in [\underline{\theta}, \bar{\theta}]$ with $\bar{\theta} = -\underline{\theta} = 2.5$. Both assumptions are verified using the ROA inner-approximation. Two types of IQCs are used to characterize the nonlinearity: an off-by-one IQC [27] to capture the slope information, and a local sector IQC to express the local sector bound.

Figure 7 shows the boundaries for the sets $\{x : v^1 \leq v^1 \leq \bar{v}^1\}$ and $\{x : \underline{\theta} \leq \theta \leq \bar{\theta}\}$ with orange and brown lines, the ROA inner-approximation with a blue ellipsoid, and some simulation trajectories with light gray dashed curves.

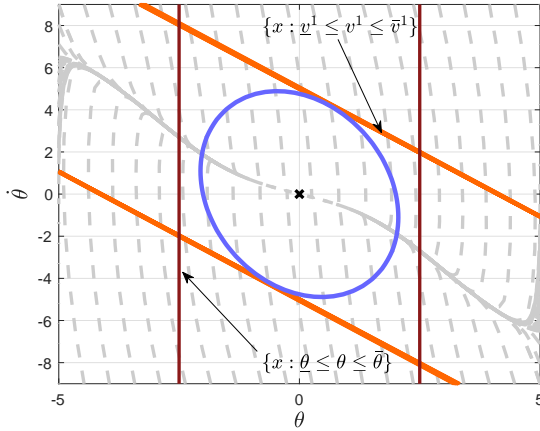


Fig. 7: A ROA inner-approximation of the inverted pendulum

B. Vehicle lateral control

Consider the vehicle lateral dynamics from [28]:

$$\begin{bmatrix} \dot{e} \\ \ddot{e} \\ \dot{e}_\theta \\ \ddot{e}_\theta \end{bmatrix} = \begin{bmatrix} 0 & 1 & 0 & 0 \\ 0 & \frac{C_{\alpha f} + C_{\alpha r}}{mU} & -\frac{C_{\alpha f} + C_{\alpha r}}{m} & \frac{aC_{\alpha f} - bC_{\alpha r}}{mU} \\ 0 & 0 & 0 & 1 \\ 0 & \frac{aC_{\alpha f} - bC_{\alpha r}}{I_z U} & -\frac{aC_{\alpha f} - bC_{\alpha r}}{I_z} & \frac{a^2 C_{\alpha f} + b^2 C_{\alpha r}}{I_z U} \end{bmatrix} \begin{bmatrix} e \\ \dot{e} \\ e_\theta \\ \dot{e}_\theta \end{bmatrix} + \begin{bmatrix} 0 \\ -\frac{C_{\alpha f}}{m} \\ 0 \\ -\frac{aC_{\alpha f}}{I_z} \end{bmatrix} u + \begin{bmatrix} 0 \\ \frac{aC_{\alpha f} - bC_{\alpha r}}{m} - U^2 \\ 0 \\ \frac{a^2 C_{\alpha f} + b^2 C_{\alpha r}}{I_z} \end{bmatrix} c \quad (35)$$

where e is the perpendicular distance to the lane edge, and e_θ is the angle between the tangent to the straight section of the

road and the projection of the vehicle's longitudinal axis. Let $x = [e, \dot{e}, e_\theta, \dot{e}_\theta]^\top$ denote the plant state. The control input u is the steering angle of the front wheel (rad), the disturbance c is the road curvature (1/m), and the parameters are: longitudinal speed of the vehicle $U = 28$ m/s, front cornering stiffness $C_{\alpha f} = -1.232 \times 10^5$ N/rad, rear cornering stiffness $C_{\alpha r} = -1.042 \times 10^5$ N/rad, vehicle mass $m = 1.67 \times 10^3$ kg, moment of inertia $I_z = 2.1 \times 10^3$ kg/m², distances from vehicle center of gravity to front axle $a = 0.99$ m and rear axle $b = 1.7$ m.

Again, the controller π is obtained through reinforcement learning using policy gradient, and is parameterized by a 2-layer, feedforward NN, with $n_1 = n_2 = 32$ and tanh as the activation function for both layers. The training process uses a discretized version of (35) with sampling time $dt = 0.02$ s and draws the curvature $c(k)$ at each time step from an interval $[-1/200, 1/200]$. The control command derived from $u(k) = \pi(x(k))$ enters the vehicle dynamics through a saturation function, defined as:

$$\text{sat}(u) := \begin{cases} u_{\max} & ; u > u_{\max}, \\ u & ; u_{\min} \leq u \leq u_{\max}, \\ u_{\min} & ; u < u_{\min}, \end{cases} \quad (36)$$

where in this case $u_{\max} = 30^\circ$ and $u_{\min} = -30^\circ$. Let $u_{\text{sat}} := \text{sat}(\pi(x))$ define the saturated control signal.

The analysis is performed for a constant curvature $c \equiv 1/200$, resulting in a non-zero equilibrium state $x_* = [-0.2865, 0, 0.0146, 0]^\top$. In the analysis problem, on top of saturation, we also add a norm-bounded LTI uncertainty $\Delta_{\text{LTI}} \in \mathbb{RH}_\infty$ with $\|\Delta_{\text{LTI}}\|_\infty \leq 0.1$ to the control input. This is used to assess the robustness of the NN controller against actuator uncertainty. As shown in Figure 8, the actual input to the vehicle dynamics is

$$u_{\text{pert}}(k) = u_{\text{sat}}(k) + q(k), \quad (37a)$$

$$q(\cdot) = \Delta_{\text{LTI}}(u_{\text{sat}}(\cdot)). \quad (37b)$$

The saturation function is static and can also be described using a local sector bound. Let \bar{u} be the largest possible control command from π induced from the assumption that $v^1 \in [\underline{v}^1, \bar{v}^1]$ where $\bar{v}^1 = v_*^1 + 0.4 \times 1_{32 \times 1}$, and $\underline{v}^1 = v_*^1 - 0.4 \times 1_{32 \times 1}$. Then the saturation function in (36) satisfies the local sector $[\alpha, \beta]$, where $\alpha := \frac{u_{\max}}{\bar{u}}$ and $\beta := 1$.

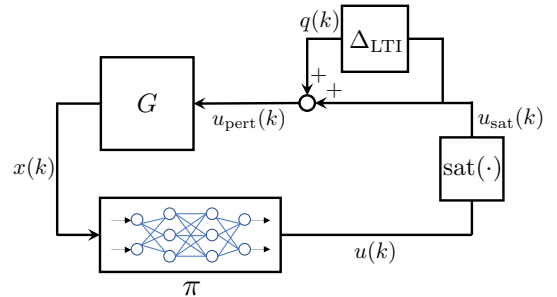


Fig. 8: Uncertain vehicle system with actuator uncertainty

The ROA inner-approximation is four dimensional. Figure 9 shows slices of this estimate on the $e-\dot{e}$ and $e_\theta-\dot{e}_\theta$ spaces. Specifically, these are intersections of $\mathcal{E}(P_x, x_*)$ with the

hyperplanes $(e_\theta, \dot{e}_\theta) = (e_{\theta*}, \dot{e}_{\theta*})$ and $(e, \dot{e}) = (e_*, \dot{e}_*)$, respectively, where $x_* = [e_*, \dot{e}_*, e_{\theta*}, \dot{e}_{\theta*}]^\top$. The slices are shown with blue ellipsoids. The boundary of the polytopic set $\{x : \underline{v}^1 \leq v^1 \leq \bar{v}^1\}$ is shown with the orange lines. The brown crosses represent the non-zero equilibrium state x_* .

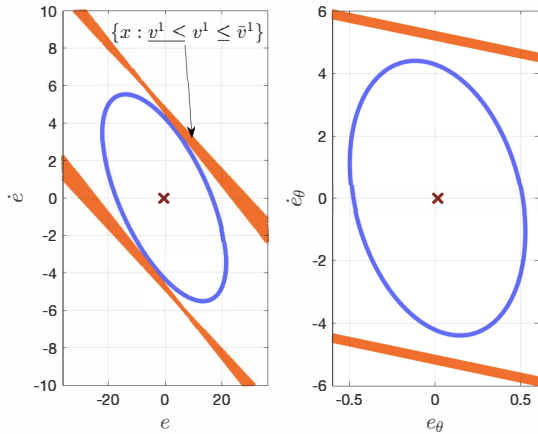


Fig. 9: Slices of the ROA inner-approximation on the $e-\dot{e}$ space and $e_\theta-\dot{e}_\theta$ spaces.

V. CONCLUSIONS

The paper presented a method to analyze stability and to inner-approximate the region of attraction of equilibria in feedback systems with NN controllers. First, LTI plants were analyzed using Lyapunov theory and local sector QCs for bounding nonlinear activation functions. Second, the results were extended to uncertain plants with perturbations described by IQCs, such as nonlinearities and unmodeled dynamics. Finally, the method was illustrated on a nonlinear inverted pendulum example, and uncertain vehicle lateral dynamics with stabilizing NN controllers obtained using policy gradient. Future work will address disturbance accommodation and reachability analysis in feedback systems with NN controllers.

VI. ACKNOWLEDGEMENTS

The authors thank Professor Andrew Packard for initiating this project. The authors also acknowledge useful discussions with Mahyar Fazlyab, Abhijit Chakraborty, and Akarsh Gupta.

REFERENCES

- [1] A. U. Levin and K. S. Narendra, "Control of nonlinear dynamical systems using neural networks: controllability and stabilization," *IEEE Transactions on Neural Networks*, vol. 4, no. 2, pp. 192–206, 1993.
- [2] R. J. Williams, "Simple statistical gradient-following algorithms for connectionist reinforcement learning," *Mach. Learn.*, vol. 8, no. 3–4, p. 229–256, May 1992. [Online]. Available: <https://doi.org/10.1007/BF00992696>
- [3] J. Peters and S. Schaal, "Reinforcement learning of motor skills with policy gradients," *Neural networks : the official journal of the International Neural Network Society*, vol. 21 4, pp. 682–97, 2008.
- [4] J. Schulman, S. Levine, P. Moritz, M. I. Jordan, and P. Abbeel, "Trust Region Policy Optimization," *arXiv e-prints*, p. arXiv:1502.05477, Feb. 2015.
- [5] S. Kakade, "A natural policy gradient," in *Proceedings of the 14th International Conference on Neural Information Processing Systems: Natural and Synthetic*, ser. NIPS'01. Cambridge, MA, USA: MIT Press, 2001, p. 1531–1538.

- [6] D. A. Pomerleau, *ALVINN: An Autonomous Land Vehicle in a Neural Network*. San Francisco, CA, USA: Morgan Kaufmann Publishers Inc., 1989, p. 305–313.
- [7] H. K. Khalil, *Nonlinear systems; 3rd ed.* Upper Saddle River, NJ: Prentice-Hall, 2002, the book can be consulted by contacting: PH-AID: Wallet, Lionel. [Online]. Available: <https://cds.cern.ch/record/1173048>
- [8] M. Vidyasagar, *Nonlinear Systems Analysis*. SIAM, 2002.
- [9] M. Fazlyab, M. Morari, and G. J. Pappas, "Safety Verification and Robustness Analysis of Neural Networks via Quadratic Constraints and Semidefinite Programming," *arXiv e-prints*, p. arXiv:1903.01287, Mar. 2019.
- [10] M. Fazlyab, A. Robey, H. Hassani, M. Morari, and G. Pappas, "Efficient and accurate estimation of Lipschitz constants for deep neural networks," in *Advances in Neural Information Processing Systems 32*. Curran Associates, Inc., 2019, pp. 11 427–11 438.
- [11] P. Pauli, A. Koch, J. Berberich, and F. Allgöwer, "Training robust neural networks using Lipschitz bounds," *arXiv e-prints*, p. arXiv:2005.02929, May 2020.
- [12] H. Hu, M. Fazlyab, M. Morari, and G. J. Pappas, "Reach-SDP: Reachability Analysis of Closed-Loop Systems with Neural Network Controllers via Semidefinite Programming," *arXiv e-prints*, p. arXiv:2004.07876, Apr. 2020.
- [13] C. Huang, J. Fan, W. Li, X. Chen, and Q. Zhu, "ReachNN: Reachability Analysis of Neural-Network Controlled Systems," *arXiv e-prints*, p. arXiv:1906.10654, Jun. 2019.
- [14] S. Dutta, X. Chen, and S. Sankaranarayanan, "Reachability analysis for neural feedback systems using regressive polynomial rule inference," in *Proceedings of the 22nd ACM International Conference on Hybrid Systems: Computation and Control*, ser. HSCC '19. New York, NY, USA: Association for Computing Machinery, 2019, p. 157–168. [Online]. Available: <https://doi.org/10.1145/3302504.3311807>
- [15] R. Ivanov, J. Weimer, R. Alur, G. J. Pappas, and I. Lee, "Verisig: verifying safety properties of hybrid systems with neural network controllers," *arXiv e-prints*, p. arXiv:1811.01828, Nov. 2018.
- [16] M. Jin and J. Lavaei, "Stability-certified reinforcement learning: A control-theoretic perspective," *arXiv e-prints*, p. arXiv:1810.11505, Oct. 2018.
- [17] K. K. Kim, E. R. Patrón, and R. D. Braatz, "Standard representation and unified stability analysis for dynamic artificial neural network models," *Neural Networks*, vol. 98, pp. 251–262, 2018.
- [18] A. Megretski and A. Rantzer, "System analysis via integral quadratic constraints," *IEEE Transactions on Automatic Control*, vol. 42, no. 6, pp. 819–830, June 1997.
- [19] J. Veenman, C. W. Scherer, and H. Köroğlu, "Robust stability and performance analysis based on integral quadratic constraints," *European Journal of Control*, vol. 31, pp. 1 – 32, 2016.
- [20] H. Hindi and S. Boyd, "Analysis of linear systems with saturation using convex optimization," in *Proceedings of the 37th IEEE Conference on Decision and Control (Cat. No.98CH36171)*, vol. 1, 1998, pp. 903–908 vol.1.
- [21] G. Zames and P. L. Falb, "Stability conditions for systems with monotone and slope-restricted nonlinearities," *SIAM Journal on Control*, vol. 6, no. 1, pp. 89–108, 1968.
- [22] W. P. Heath and A. G. Wills, "Zames-Falb multipliers for quadratic programming," in *Proceedings of the 44th IEEE Conference on Decision and Control*, 2005, pp. 963–968.
- [23] A. Iannelli, P. Seiler, and A. Marcos, "Region of attraction analysis with integral quadratic constraints," *Automatica*, vol. 109, p. 108543, 2019.
- [24] H. Yin, P. Seiler, and M. Arcak, "Backward Reachability using Integral Quadratic Constraints for Uncertain Nonlinear Systems," *arXiv e-prints*, p. arXiv:2003.05617, Mar. 2020.
- [25] H. Yin, A. Packard, M. Arcak, and P. Seiler, "Reachability Analysis Using Dissipation Inequalities For Uncertain Nonlinear Systems," *arXiv e-prints*, p. arXiv:1808.02585, Aug. 2018.
- [26] F. Berkenkamp, R. Moriconi, A. P. Schoellig, and A. Krause, "Safe learning of regions of attraction for uncertain, nonlinear systems with gaussian processes," in *2016 IEEE 55th Conference on Decision and Control (CDC)*, 2016, pp. 4661–4666.
- [27] L. Lessard, B. Recht, and A. Packard, "Analysis and design of optimization algorithms via integral quadratic constraints," *SIAM Journal on Optimization*, vol. 26, no. 1, pp. 57–95, 2016.
- [28] A. Alleyne, "A comparison of alternative intervention strategies for unintended roadway departure (urd) control," *Vehicle System Dynamics*, vol. 27, no. 3, pp. 157–186, 1997.